Neoplasia • Vol. 9, No. 11, November 2007, pp. 938–950 938

www.neoplasia.com

Origin of Androgen-Insensitive Poorly Differentiated Tumors in the Transgenic Adenocarcinoma of Mouse Prostate Model[1,2]

Wendy J. Huss, Danny R. Gray[†], Keyvan Tavakoli[‡], Meghan E. Marmillion[‡], Lori E. Durham[‡], Mac A. Johnson[§], Norman M. Greenberg[¶] and Gary J. Smith*[,‡]*

*Department of Urologic Oncology, Roswell Park Cancer Institute, Buffalo, NY 14263, USA; [†]Center for Vascular Biology Research, Division of Molecular and Vascular Medicine, Beth Israel Deaconess Medical Center, Boston, MA, USA; [‡]Department of Pathology and Laboratory Medicine, University of North Carolina at Chapel Hill, Chapel Hill, NC, USA; [§]Imaging Sciences, Vertex Pharmaceuticals, Cambridge, MA, USA; [¶]Clinical Research Division, Fred Hutchinson Cancer Research Center, Seattle, WA, USA

Abstract

Following castration, the transgenic adenocarcinoma of mouse prostate (TRAMP) model demonstrates rapid development of SV40-Tag–driven poorly differentiated tumors that express neuroendocrine cell markers. The cell population dynamics within the prostates of castrated TRAMP mice were characterized by analyzing the incorporation of 5-bromodeoxyuridine (BrdUrd) and the expression of SV40-Tag, synaptophysin, and androgen receptor (AR). Fourteen days postcastration, the remaining epithelial cells and adenocarcinoma cells were nonproliferative and lacked detectable SV40-Tag or synaptophysin expression. In contrast, morphologically distinct intraglandular foci were identified which expressed SV40-Tag, synaptophysin, and Ki67, but that lacked AR expression. These proliferative SV40-Tag and synaptophysin-expressing intraglandular foci were associated with the rare BrdUrd-retaining cells. These foci expanded rapidly in the postcastration prostate environment, in contrast to the AR– and SV40-Tag–expressing adenocarcinoma cells that lost SV40-Tag expression and underwent apoptosis after castration. Intraglandular foci of synaptophysin-expressing cells were also observed in the prostates of intact TRAMP mice at a comparable frequency; however, they did not progress to rapidly expanding tumors until much later in the life of the mice. This suggests that the foci of neuroendocrine-like cells that express SV40-Tag and synaptophysin, but lack AR, arise independent of androgen-deprivation and represent the source of the poorly differentiated tumors that are the lethal phenotype in the TRAMP model.

Neoplasia (2007) **9,** 938–950

Keywords: Prostate cancer, androgen-insensitive, TRAMP, neuroendocrine, synaptophysin.

Introduction

The essentially inevitable recurrence of prostate cancer (castration-recurrent prostate cancer) that follows androgen-deprivation therapy (castration) suggests that the prostatic response to castration may prime a component of the tumor for progression to castration-recurrent disease. One possibility is that androgen-insensitive neuroendocrine (NE) cells signal through the release of growth and survival factors to the prostate tumor stem cell that also survives androgen-deprivation therapy, promoting a stem cell–fed emergence of castration-recurrent disease. NE cells are observed in 50% to 100% of primary prostate cancers and metastases, and the number of NE cells correlates with stage, Gleason Grade, and survival in castration-recurrent prostate cancer [1–3]. However, the origin of tumor-associated NE cells in castration-recurrent prostate cancer is unclear. Two potential sources of the NE compartment in castration-recurrent prostate cancer are: 1) progeny of prostate tumor stem cells that undergo *terminal* NE differentiation in the androgen-deprived environment; or 2) transdifferentiation of adenocarcinoma cells into NE-like cells.

In the transgenic adenocarcinoma of the mouse prostate (TRAMP) model, the −426/+28 minimal rat probasin promoter (rPB) provides androgen-regulated expression of SV40-Tag in the epithelium of the mouse prostate. The TRAMP transgene in a C57BL/6 × FVB background causes the appearance of androgen receptor (AR)–expressing adenocarcinomas in the majority of prostate glands by 16 weeks of age. However, the poorly differentiated tumors that ultimately kill TRAMP, and 9/23 (39%) lymph node metastases, but the primary tumors, expressed synaptophysin [4,5], a widely used marker of NE

Abbreviations: TRAMP, transgenic adenocarcinoma of mouse prostate; AR, androgen receptor; NE, neuroendocrine; GEM, genetically engineered mouse; rPB, rat probasin promoter; PSA, prostate-specific antigen; AMACR, α-methylacyl-CoA racemase; PIN, prostatic intraductal *neoplasia*; BrdUrd, 5-bromodeoxyuridine

Address all correspondence to: Wendy J. Huss, Roswell Park Cancer Institute, 142 C&V Annex, Elm and Carlton Streets, Buffalo, NY 14263, USA. E-mail: wendy.huss@roswellpark.org

[1]This work was supported by CA77739 (G.J.S.), CA84296 (N.M.G.), and CA64851 (N.M.G.), by Roswell Park Cancer Institute Alliance Foundation (W.J.H.), and by W81XWH-04-0020 (W.J.H.).

[2]This article refers to supplementary material, which is designated by Figure W1 and is available online at www.bcdecker.com.

Received 5 July 2007; Revised 13 September 2007; Accepted 17 September 2007.

DOI 10.1593/neo.07562

differentiation in mouse and human prostate and CaP [3,6,7]. Furthermore, many of the SV40-Tag–based genetically engineered mouse (GEM) models of prostate cancer also develop rapidly progressing, poorly differentiated tumors that express synaptophysin and other NE cell markers [8]. In TRAMP, castration accelerated (or synchronized) the independent emergence of highly proliferative, poorly differentiated tumors that expressed synaptophysin, but had low or undetectable levels of AR: these tumors, not the more prevalent adenocarcinomas, ultimately killed the host [9]. Poorly differentiated primary or metastatic tumors were found in up to 93% of 24-week-old TRAMP mice in the C57BL/6 × FVB background that had been castrated at 12 weeks of age [5,10], whereas 100% of intact TRAMP at 38 weeks of age mice displayed poorly differentiated tumors [11]. Following castration at 15 weeks of age, there was only 50% survival at 27 weeks of age, with no survival at 30.5 weeks of age, whereas 60% of 27-week-old and 30% of 30.5-week-old intact TRAMP mice in the C57BL/6 × FVB background survived [9]. Castration, therefore, functionally synchronizes mortality in a subset of TRAMP mice by accelerating or by facilitating emergence of the poorly differentiated tumors.

The well-differentiated adenocarcinomas present in intact TRAMP mice responded to castration with cessation of proliferation, induction of apoptosis, and loss of AR-mediated transactivation, including loss of expression of SV40-Tag. In contrast, the poorly differentiated tumors within the prostate, or at sites of metastases, demonstrated no changes in proliferative or apoptotic indices, and maintained expression of SV40-Tag at 3 days postcastration, the only postcastration time point examined before the development of palpable tumors in TRAMP mice in the C57BL/6 background [12]. Well-differentiated adenocarcinomas and poorly differentiated tumors differ markedly in expressed signaling molecules, in the expression of markers of differentiation, rates of proliferation and apoptosis, vessel density, and in androgen responsiveness [5,12–17]. With the exception of the study performed by Wikstrom et al. [12], the response of poorly differentiated tumors in TRAMP to androgen-deprivation has been analyzed only in the context of large poorly differentiated tumors [5,9,10], precluding elucidation of the origin of the these tumors.

Several *in vitro* and *in vivo* models support the hypothesis of a bidirectional transdifferentiation of prostate cancer cells into NE cells, particularly in response to androgen-deprivation [18–20]. Treatment of LNCaP cells with reagents that raise intracellular levels of cAMP, or enzyme inhibitors that block degradation of cAMP, or by removal of steroids from the culture media induced LNCaP cells to assume a neuronal morphology; produce more chromogranin A; secrete bombesin-, serotonin-, and neuron-specific enolase; and cease expression of AR and secretion of prostate-specific antigen (PSA) [18,21–24]. Castration of mice bearing the LNCaP tumor resulted in a 15-fold increase in the number of NE cells within 4 weeks [21]. Finally, the PC-295 and PC-310 human prostate cancer xenografts underwent extensive neuroendocrine differentiation (up to 50% of the prostate cancer cells) in response to castration of the mouse host in the apparent absence of cellular proliferation [25–27].

Tracking label retention following long-term *pulse – chase* labeling with 5-bromodeoxyuridine (BrdUrd) can determine the origin of NE cells by lineage tracing of the differentiated progeny of progenitor cells, and/or by demonstration of the transdifferentiation of mature epithelial cells into NE cells. Infrequently, proliferating progenitor/stem cells have been identified as label-retaining cells in many organs, including the proximal region of the mouse ventral prostate [28], using BrdUrd retention to identify cells that replicate during the BrdUrd pulse period and remain quiescent for extended intervals during the chase. Whereas quiescent progenitor/stem cell retain BrdUrd label, the highly proliferative progeny of the stem cell/tumor stem cell (the transit-amplifying compartment) rapidly dilutes the incorporated BrdUrd with successive cell divisions to a level below detection [28]. In fact, BrdUrd retention was used to demonstrate that transdifferentiation of adenocarcinoma cells to NE cells in the absence of proliferation was responsible for neuroendocrine differentiation elicited in response to castration in the PC-295 human prostate cancer xenograft [26]. NE cells in benign prostate are believed to derive from the prostate epithelial stem cell, not the neural crest [29,30]. However, in prostate cancer, the origin of NE cells is unclear. In CaP, NE cells have been observed to coexpress α-methylacyl-CoA racemase (AMACR), a tumor cell marker, and chromogranin A [31], a neuroendocrine marker, suggesting that either AMACR-expressing prostate tumor cells can acquire the ability to express NE markers through transdifferentiation or NE cells within areas of prostate cancer can express AMACR. Because increased levels of NE differentiation is a characteristic of castration-recurrent CaP, identification of the mechanism responsible for the appearance of the NE cells in response to androgen-deprivation could provide important insights into the biology of the lethal form of the disease.

This study was initiated to identify the origin and role of the NE marker–expressing cells in poorly differentiated cancers in TRAMP and to determine if the TRAMP model can enhance our understanding of the origin and contributions of the NE compartment to the pathogenesis of castration-recurrent human prostate cancer. This study suggests that NE marker–expressing cells in the poorly differentiated TRAMP tumors emerge independent from the adenocarcinomas and derive from malignantly transformed progenitor cells rather than from transdifferentiation of adenocarcinoma cells.

Materials and Methods

TRAMP Model

All experiments using laboratory animals were performed in accordance with the Institutional Animal Care and Use Committee and the National Institutes of Health guidelines. Male TRAMP mice [C57BL/6 TRAMP × FVB] $F1^{+/-}$ were obtained from the colony maintained in the laboratory of Norman Greenberg at the Baylor College of Medicine and a colony at Taconic Laboratories. Mice were bred and genotypically screened as described [5,9].

Fourteen-week-old TRAMP mice in the C57BL/6 × FVB background were either castrated by radical orchiectomy or sham-castrated through a scrotal incision, with a single suture used to close the incision (10 animals/time point). The dorsal, lateral, and ventral lobes of the prostate, pelvic lymph nodes, small intestine, and any grossly apparent metastases were harvested at 0, 1, 2, 4, 7, and 14 days postcastration/sham.

BrdUrd incorporation experiments to trace the role of proliferation in NE-differentiation were performed in a subset of animals (five animals/time point). Male TRAMP mice were implanted with minipumps (Alzet; Durect Corp., Cupertino, CA) that contained 200 μl of BrdUrd (60 mg/ml; Sigma, St. Louis, MO) at 12 weeks of age, and the minipumps were maintained for 2 weeks to provide continuous BrdUrd release. Two days after pump removal, mice were castrated or sham-castrated and tissue specimens were harvested at the time points described above.

BrdUrd incorporation experiments to identify persistent label-retaining cells were performed in TRAMP mice that were 14 weeks old at the time of castration (n = 6 castration; n = 6 sham castration). Male TRAMP were castrated or sham-castrated, implanted with BrdUrd minipumps (as described above), and maintained for 2 weeks. The pumps were removed and the animals were maintained for a *chase* in the absence of BrdUrd for 4 weeks (42 days postcastration/sham). Dorsal, lateral, and ventral prostates, pelvic lymph nodes, small intestine, and any macroscopic metastases were harvested at 20 weeks of age.

Tissues collected at necropsy from each animal were fixed in 10% neutral-buffered formalin (Sigma) for 24 hours in a single multichamber cassette, transferred to 70% ethanol, and embedded in a single paraffin block. Prostate lobes were completely sectioned at 5-μm intervals and sections were mounted on slides (ProbeOn-Plus; Fisher, Raleigh, NC).

Immunohistochemistry

Prostate and other tissues from TRAMP mice were processed, and immunohistochemical (IHC) analyses performed as described [32]. Briefly, slides were deparaffinized in xylene, rehydrated through a graded series of alcohol washes, and equilibrated in PBS. For Foxa1 and Foxa2 antibodies, antigen retrieval was performed in 10 mM citric acid, pH 6.0, for 30 minutes at 95°C in a steamer, or for antibodies for AR, synaptophysin, Ki67, SV40-Tag, ABCG2, and serotonin by continuous boiling in a microwave. Antigen retrieval for the BrdUrd antibody was performed by incubating in 5 U/ml DNase (Sigma) in Tris–boric acid–saline solution, pH 7.5, for 30 minutes at 37°C. Slides were incubated with appropriate primary antibodies: 1:100 dilution of rabbit polyclonal anti-AR (Calbiochem, San Diego, CA); 1:20 dilution of rat monoclonal anti-ABCG2 (Bxp-53) (Caltag Laboratories, Burlingame, CA) [33]; 1:600 dilution of rabbit polyclonal anti-synaptophysin (Zymed Laboratories, South San Francisco, CA); 1:250 dilution of mouse monoclonal anti-BrdUrd (Sigma); 1:1000 dilution of rabbit polyclonal anti-Ki67 (Novocastra Laboratories, New Castle, UK); 1:100 dilution of mouse monoclonal anti–SV40-Tag (BD Pharmingen, San Diego, CA); 1:250 dilution of rabbit polyclonal anti-serotonin (ICN, Immunobiologics, Irvine, CA); 1:100 dilution of goat polyclonal anti-Foxa1 (Santa Cruz, Santa Cruz, CA); 1:100 dilution of goat polyclonal anti-Foxa2 (Santa Cruz) for 30 minutes at 37°C. All slides were incubated with the appropriate biotinylated secondary antibody: goat anti–rabbit IgG (Vector, Burlingame, CA); rabbit anti–rat IgG (Vector); goat anti–mouse IgG (Vector); or rabbit anti–goat IgG (Jackson ImmunoResearch Laboratories, Inc., West Grove, PA) at a 1:1000 dilution for 20 minutes at 37°C. Immunoreactive antigens were detected using the Vectastain Elite ABC Immunoperoxidase Kit and DAB, Nova Red (Vector), TrueBlue (KPL, Gaithersburg, MD), or ABC Alkaline Phosphatase Kit I or III (Vector). Omission of primary antibody, and tissue from animals not injected with BrdUrd (for BrdUrd staining), served as negative controls, and positive control tissues (small intestine for BrdUrd, Ki67, synaptophysin, and ABCG2 staining, and prostate from intact TRAMP mouse for SV40 and AR staining) were included for each experiment.

Quantitative and Statistical Analysis

The percent of cells that demonstrated SV40-Tag expression, proliferation, apoptosis, and BrdUrd incorporation was determined by counting the number of epithelial cells that stained positive for SV40-Tag, Ki67, activated caspase-3, or BrdUrd, and the total number of epithelial cells detected by morphology, in two to three representative 100× fields from five animals/time point for tissue from the dorsal, lateral, and ventral prostate lobes (average of 1000 epithelial cells/lobe). Blood vessels were identified by staining endothelial cells with CD31 and ABCG2, as described [14,32] in two to three representative 100× fields from five animals/time point. Blood vessels were counted and the perimeters were measured with ImageJ software (NIH, Bethesda, MD) [34]. Means, standard error, and one-way nonparametric ANOVA tests were performed using Prism software (GraphPad, San Diego, CA).

Results

Expression of SV40-Tag Transgene in Prostate of Castrated TRAMP Mice

SV40-Tag expression was evaluated in the three prostate lobes (dorsal, lateral, and ventral) to determine changes in epithelial SV40-Tag expression in response to castration. The SV40-Tag index (Figure 1) was calculated in prostate tissue specimens (benign prostate, prostatic intraductal *neoplasia* (PIN), and well-differentiated adenocarcinoma were analyzed together, whereas poorly differentiated tumors were analyzed separately, and are discussed below). SV40-Tag protein was expressed in 90% of the epithelial cells in the dorsal, lateral, and ventral lobes of the prostate before castration, and expression was maintained at comparable levels in sham castration (control) TRAMP mice. In castrated mice, the percent of epithelial cells that expressed SV40-Tag was decreased significantly in all lobes of the prostate on Day 2 postcastration, compared to prostates from sham-castrated animals ($P < .005$), and continued to decrease over the ensuing interval following castration (Figure 1, *A*–*G*). SV40-Tag was expressed in less than 1% of epithelial cells

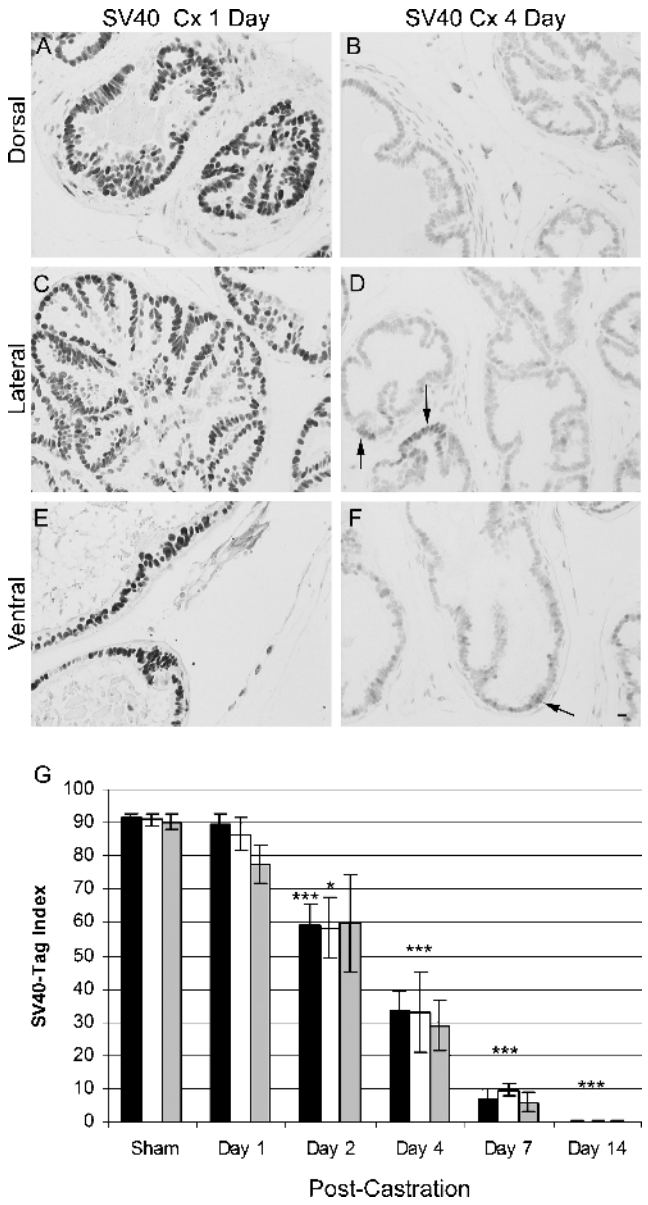

Figure 1. *Epithelial cell expression of SV40-Tag in TRAMP prostates following castration (Cx). Dorsal prostate Day 1 postcastration (A) and Day 4 postcastration (B); Lateral prostate Day 1 postcastration (C) and Day 4 postcastration (D); Ventral prostate Day 1 postcastration (E) and Day 4 postcastration (F) immunostained for SV40-Tag. (G) The percent of epithelial cells expressing SV40-Tag in each lobe of the prostate ■ dorsal, □ lateral, and ■ ventral. ***P < .001: Days 4, 7, and 14 postcastration compared to sham-castrated animals in all lobes and Day 2 postcastration in the dorsal lobe only. *P < .05: Day 2 postcastration compared to sham castration in the lateral lobe.* Black arrows*, SV40-Tag–expressing cells Day 4 postcastration. Scale bar, 20 μm.*

in all lobes on Day 14 postcastration and, in the ventral prostate, was observed only in focal areas or in poorly differentiated tumors.

Proliferation and Apoptotic Indices of Prostate Epithelial Cells following Castration

Expressions of Ki67, a marker of proliferation, and of activated caspase-3, a marker of apoptosis, were evaluated to determine the proliferative and apoptotic response to castration in epithelial cells in the three prostate lobes. The proliferation and apoptotic indices were quantitated in prostate tissues (normal, PIN, and well-differentiated adenocarcinoma were analyzed together, whereas poorly differentiated tumors were analyzed separately, and are discussed below). The proliferation index in the dorsal and lateral lobes was decreased significantly (2-fold) at Day 2 postcastration compared to prostates from control animals ($P < .05$) (Figure 2*A*). Furthermore, the proliferation index in the ventral lobe was decreased by more than 7-fold at Day 2 postcastration compared to prostates from control mice ($P < .05$). The proliferation index for all three lobes was reduced to less than 1.5% of levels in sham castration mice on Day 14 of postcastration.

Expression of activated caspase-3 increased in the prostate between Days 1 and 4 postcastration (Figure 2*B*). The apoptotic index increased 4-fold in the dorsal and lateral lobes ($P < .01$) and increased 5-fold in the ventral lobe ($P < .005$) on Day 1 postcastration compared to the corresponding prostate lobes from control mice (Figure 2*B*). The apoptotic index increased 2-fold in the dorsal and lateral lobes ($P < .01$) on Days 2 and 4 postcastration compared to

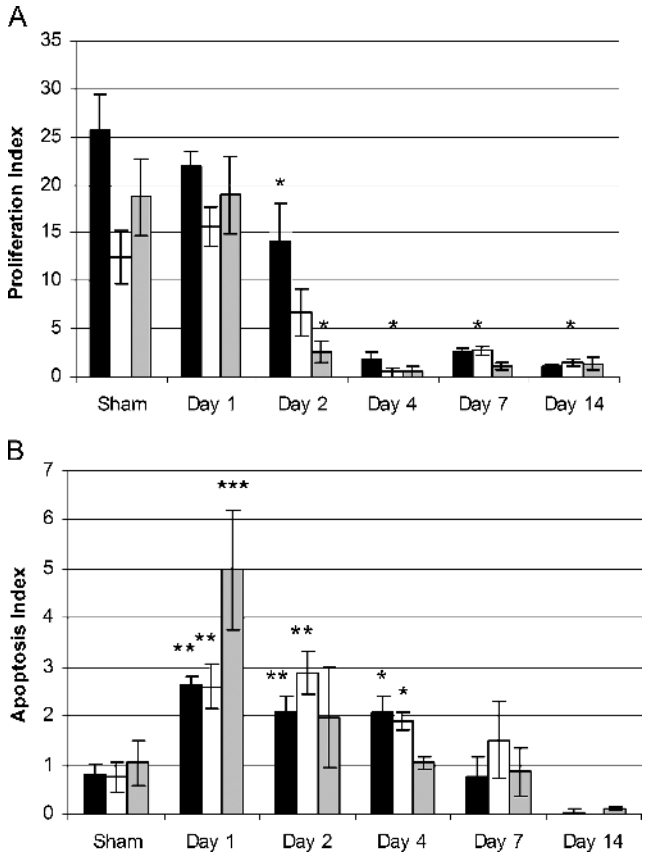

Figure 2. *Epithelial cell proliferation and apoptosis in TRAMP prostates following castration. (A) The percent of proliferation in epithelial cells in each lobe of the prostate ■ dorsal, □ lateral, and ■ ventral. *P < .05: Days 4, 7, and 14 postcastration compared to sham-castrated animals in all lobes and Day 2 postcastration in the dorsal and ventral lobes only. (B) The percent of apoptosis in epithelial cells in each lobe of the prostate ■ dorsal, □ lateral, and ■ ventral. ***P < .001: Day 1 postcastration compared to sham-castrated animals in ventral lobe. **P < .01: Days 1 and 2 postcastration compared to sham-castrated animals in dorsal and lateral lobes. *P < .05: Day 4 postcastration compared to sham-castrated animals in dorsal and lateral lobes.*

the prostate lobes from control mice (Figure 2*B*). The percent of cells undergoing apoptosis at Day 7 postcastration had returned to sham castration levels. The ventral lobe of the prostate, which demonstrated the most dramatic change (> 6-fold decrease) in proliferation index in response to castration on Day 2 through Day 14 postcastration compared to the ventral lobes from control mice, also demonstrated the greatest increase in apoptosis index after castration (Figure 2, *A* and *B*).

Vascular Changes in TRAMP Prostate following Castration

The response of the prostatic vasculature to castration was characterized by quantifying the number of blood vessels per microscope field in prostate tissues characterized as normal epithelium, PIN, and well-differentiated adenocarcinoma (Table 1). Vascular changes in the large poorly differentiated tumors were analyzed separately; they are discussed in a later section. The perimeters of the blood vessels were traced in the same fields used for quantification, the total length of the perimeters of the blood vessel per field was determined, and the average perimeter per vessel was calculated for each time point postcastration (Table 1). No significant differences in blood vessel density or average vessel perimeter were observed between the three prostate lobes at any time point (data not shown), therefore, the reported values represent an average of the three lobes. There was a significant increase in the density of blood vessels on Day 14 postcastration compared to the blood vessel density in prostates from control mice ($P < .05$) (Table 1). However, there was no significant difference in the perimeter of the blood vessels between castrated and sham-castrated TRAMP animals across the postcastration time points (Table 1). The increased number of blood vessels in Day 14 postcastration without an increase in total vessel perimeter suggests that the new blood vessels are smaller postcastration, and possibly are the result of active angiogenesis.

BrdUrd Retention Used to Examine Proliferation/ Differentiation following Castration

In the initial series of BrdUrd label-retention experiments, TRAMP mice were implanted with BrdUrd-filled osmotic pumps at 12 weeks of age, the pumps removed following 2 weeks of continuous BrdUrd infusion and, 2 days following pump removal, mice were castrated or sham-castrated. Long-term retention of BrdUrd was used to track the dynamics of prostate cell populations following castration. The central goal of the study was to determine whether the emergence of synaptophysin-expressing cells that comprised the poorly differentiated tumors was the result of differentiation of the progeny of a prostate label–retaining cell, requiring multiple cell divisions during progression through the transit-amplifying compartment, or was the result of transdifferentiation from an adenocarcinoma cell, without cell division. BrdUrd label was present in almost all epithelial cells of the highly proliferative small intestine used as a positive control at the time of castration (Day 0, data not shown). However, BrdUrd label was diluted from intestinal epithelial cell nuclei by the rapid proliferation that occurred over the days that followed removal of the osmotic pump (data not shown). The percentage of intestinal epithelial cells that retained BrdUrd label was related inversely to the rate of proliferation of the cells that had incorporated BrdUrd during the pulse period. In contrast, only 5% to 9% of adenocarcinoma cells in the prostates of TRAMP mice demonstrated BrdUrd incorporation at the time of castration (Figure 3), suggesting a relatively low rate of proliferation. At Day 14 postcastration, BrdUrd label was retained in 2-fold more tumor cells in the lateral and ventral prostates compared to sham-castrated control mice (Figure 3) reflecting the reduced rate of proliferation in the absence of circulating androgens. In contrast, in the poorly differentiated tumors that emerge after castration, < 0.2% of cells retained label after the 16-day chase, reflecting the high rate of proliferation in these cells.

Table 1. Changes in TRAMP Prostate Vasculature following Castration.

No. of Days Postcastration	Blood Vessel Density (No./Field)	Blood Vessel Perimeter (μm/Field)
0	13.03 ± 1.35	74.09 ± 5.31
1	10.47 ± 0.92	89.44 ± 7.07
2	13.58 ± 1.82	72.86 ± 6.72
4	13.52 ± 0.89	69.82 ± 2.74
7	14.37 ± 1.00	72.09 ± 4.35
14	18.16* ± 2.054	68.07 ± 3.83

*$P < .05$ compared to sham-castrated TRAMP mice.

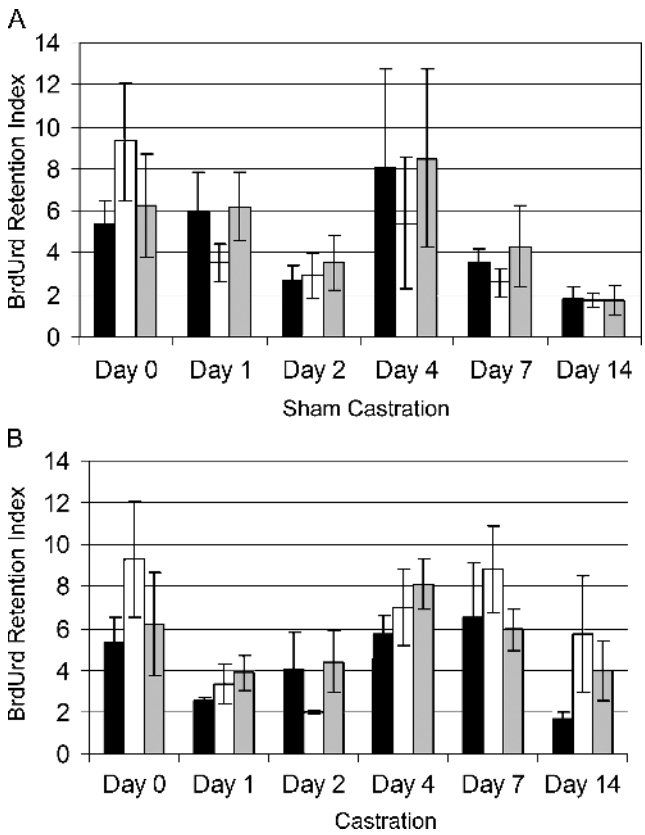

Figure 3. *BrdUrd retention in epithelial cells in TRAMP prostates following castration ■ dorsal, □ lateral, and ■ ventral lobes of the prostate from animals sham-castrated (A) or castrated (B).*

There was no evidence of synaptophysin-expressing, BrdUrd-positive cells in either intact or castrated animals. This observation suggested that synaptophysin-expressing cells were the result of proliferation and differentiation of progeny of a progenitor cell and not transdifferentiation of an adenocarcinoma cell. Therefore, the incidence of synaptophysin-expressing cells (single cell or foci of cells) in the ventral prostate per slide was determined (Table 2). Synaptophysin-expressing cells located within the basement membrane of the glands (intraglandular) were quantitated as two separate categories: foci of one to two cells that expressed synaptophysin (Figure 4*A*) or foci of more than two cells that expressed synaptophysin (Figure 4, *B* and *C*). Synaptophysin-expressing/BrdUrd-negative cells present on Day 1 postcastration, after 3 days of chase (BrdUrd removal), were observed at the same frequency in intact and castrate animals, supporting that the synaptophysin-expressing cells were highly proliferative in both intact and castrated animals (Figures 5*A* and 6*A*), or were present at the time of castration but were not proliferative during the pulse period (Figure 4, *A* and *B*). However, rare synaptophysin-expressing foci associated with BrdUrd-retaining cells on the periphery of the foci suggest that the synaptophysin-expressing foci derive from label-retaining cells (Figure 4*C*).

Synaptophysin-Expressing Foci and Tumors in TRAMP Ventral Prostates

Synaptophysin-expressing cells were associated with three pathologies in the ventral prostate of both intact and castrated TRAMP mice (Figures 5 and 6): foci localized within glands (intraglandular foci) (*A*); microscopic tumors, invasive tumor that was not visible grossly on dissection (*B*); and macroscopic tumors, visible on dissection (*C*). Serial sections containing these synaptophysin-expressing foci/tumors were examined by IHC for coexpression of: SV40-Tag (Figures 5, *D–F* and 6, *D–F*); AR and ABCG2, a putative progenitor cell marker (Figures 5, *G–I* and 6, *G–I*); Foxa2, a transit-amplifying cell marker (Figures 5, *J–L* and 6, *J–L*); serotonin, a NE cell marker (Figure W1, *A–C*); and Foxa1, an epithelial cell marker (Figure W1, *D–F*). Metastases in pelvic lymph nodes from the same mice (when present) are shown in the insets. In general, all synaptophysin-expressing, poorly differentiated foci and tumors coexpressed SV40-Tag, Foxa1, and Foxa2 and had high levels of proliferation as detected with Ki67. Rare intraglandular foci (1/24), microscopic tumors (1/14), and macroscopic tumors (2/19) that expressed synaptophysin, but not Foxa2, were detected, in both intact and castrated animals (Table 2). AR expression was detected in a few synaptophysin-expressing foci and tumors from intact and castrated animals, and AR expression was usually correlated with a lack of Foxa2 expression (Table 2). AR expression was detected in a single lymph node metastasis (Figure 5*G*, *inset*) in an intact animal; the lymph node metastasis coexpressed synaptophysin and SV40-Tag (Figure 5, *A* and *D*), but not Foxa2 (Figure 5*J*). This metastasis possibly represents a rare instance of AR, not Foxa2 driving the probasin promoter in a synaptophysin-expressing metastatic tumor.

Prostates from castrated TRAMP demonstrated AR expression in the cytoplasm of adenocarcinoma cells on Days 1 and 4 postcastration (Figure 6*G*), but AR expression was nuclear beginning at Day 7 postcastration (data not shown), and AR expression remained nuclear at Day 14 postcastration (Figure 6*H*). The percent of luminal epithelial cells that expressed SV40-Tag decreased after castration, until SV40-Tag expression was not detectable on Day 14 postcastration, even in epithelial cells that had regained nuclear AR expression (Figure 6, *E* and *H*). Synaptophysin-expressing cells in foci, or in tumors, were the only cells in castrate prostates that expressed SV40-Tag and Ki67 on Day 7 and Day 14 following castration (Figure 6, *B* and *E*). Serotonin coexpression with synaptophysin was observed in ~ 27% of the intraglandular foci following castration (Figure W1*G*; Table 2), and was also observed in 15% of intraglandular synaptophysin-expressing foci from intact TRAMP; however, coexpression of serotonin was never detected in microscopic or macroscopic tumors (Figure W1, *E–F* and *H–I*). Foxa1 was expressed in synaptophysin-expressing foci and tumors, but was expressed intensely in synaptophysin-negative cells (Figure W1, *J–L*). The coexpression of synaptophysin, Foxa2, SV40-Tag, and Ki67 in the intraglandular foci, microscopic

Table 2. Incidence of Synaptophysin- or Foxa2-Expressing Cells in TRAMP Prostates.

	No Foci		Intraglandular Synaptophysin or Foxa2$^+$, 1–2 Isolated Cells		Intraglandular Synaptophysin or Foxa2$^+$, > 2 Cells (Foci)		Microscopic Tumor		Macroscopic Tumor	
	Intact	Cx	Intact	Cx	Intact	Cx	Intact	Cx	Intact	Cx
No. of animals	17	19	5	4	6	10	11	7	3	11
Frequency of Synaptophysin$^+$ or Foxa2$^+$/Slide	26/65 (0.4)	33/82 (0.4)	8/65 (0.12)	9/82 (0.08)	18/65 (0.28)	16/82 (0.2)	14/65 (0.22)	9/82 (0.11)	5/65 (0.08)	17/82 (0.21)
No. of LN Metastasis/ Animal$^{-/+}$/NA	8/1/8	9/1/9	2/0/3	1/0/3	5/1/0	7/1/2	3/0/8	4/0/3	0/3/0	3/4/4
Frequency of Serotonin$^+$/Foci	NA	NA	Not found on serial slides		2/13	3/11	0	0	0	0
Frequency of Foxa2$^-$/Foci	NA	NA	Not found on serial slides		1/13	0	0	1/6	1/4	1/15
AR$^+$/Foci	NA	NA	Not found on serial slides		3/13	0	4/8	1/6	2/4	1/15

There is a significant difference in the number of animals with different pathologies between intact and castrated (Cx) TRAMP in these defined categories with $P < .05$, chi-square analysis. The frequency of serotonin$^+$, Foxa2$^-$, and AR$^+$ is per synaptophysin-expressing foci.

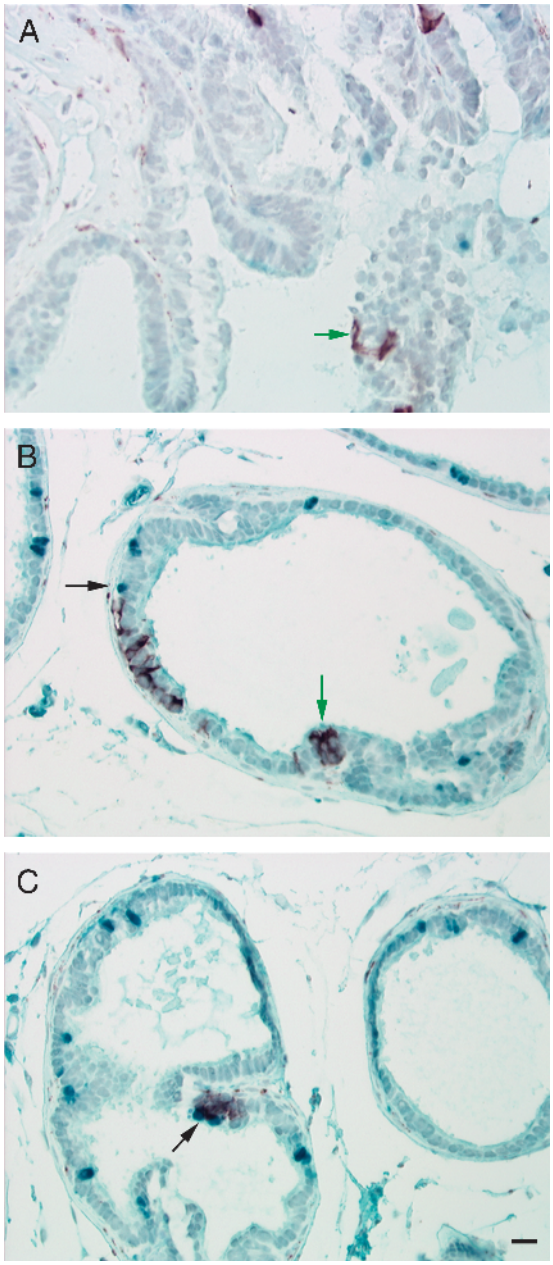

Figure 4. *BrdUrd retention in synaptophysin-expressing intraglandular foci. Ventral prostate Day 1 postcastration and Day 3 post–BrdUrd removal (A and B); Day 4 postcastration and Day 6 post–BrdUrd removal (C); immunostained for BrdUrd – blue and synaptophysin – red. BrdUrd label–retaining cells (black arrows) and synaptophysin-expressing cells (green arrows) postcastration. Scale bar, 20 μm.*

tumors, and macroscopic tumors from intact and castrated TRAMP mice suggest an index phenotype for the emerging poorly differentiated tumors unique from the adenocarcinomas, particularly in the castrate prostate.

The incidence of intraglandular, isolated synaptophysin-expressing cells and of foci of synaptophysin-expressing cells, microscopic tumors, and macroscopic tumors was calculated for the ventral prostates from intact and castrated TRAMP mice. All ventral prostates without macroscopic tumors were sectioned completely, and sections spaced at 25-μM intervals were examined by IHC analysis for the expression of Foxa2, synaptophysin, and SV40-Tag (Table 2). A significant difference (chi-square analysis) was observed for the total number of foci and tumors between intact and castrated TRAMP mice ($P < .05$). However, there was no statistical difference between intact and castrated animals when comparing the individual types of foci or tumors. The proliferation and apoptotic indices, the blood vessel density, and the length of vessel perimeter per field were calculated in intraglandular synaptophysin-expressing foci and in both microscopic and macroscopic tumors (Table 3). There was no difference in blood vessel density, length of vessel perimeter, and proliferation or apoptotic indices between cells in the intraglandular synaptophysin-expressing foci and tumors in sham-castrated and in castrated TRAMP mice (Table 3). Based on marker expression, the pattern of proliferation, and the expression of synaptophysin following castration, the intraglandular foci could represent the precursor to the microscopic and macroscopic tumors that arise rapidly after castration.

Metastasis

Pelvic lymph nodes were harvested and examined for evidence of metastasis. The majority of pelvic lymph node metastases were found in animals that had macroscopic tumors. The metastatic cells expressed synaptophysin, SV40-Tag, and Foxa2 and lacked detectable levels of AR. However, metastases were observed in both intact and castrated animals that lacked synaptophysin, and a single metastasis that expressed synaptophysin, SV40-Tag, and detectable AR, but not Foxa2, was detected in an intact animal that had an intraglandular synaptophysin-expressing foci, but no microscopic or macroscopic tumors within the ventral prostate (Figure 5, *A*, *D*, *G*, and *J*).

Label-Retaining Cells following Castration

A second BrdUrd-based experimental format was employed to examine the origin of synaptophysin-expressing cells that become apparent after castration. TRAMP mice were implanted with osmotic pumps containing BrdUrd and were either castrated or sham-castrated. The pumps were removed following 2 weeks of continuous BrdUrd labeling, the animals were maintained for a 2-week chase period, and tissues were harvested. Macroscopic tumors were present in 3/6 castrated mice (1/6 with positive pelvic lymph nodes) and 1/6 sham-castrated mice (1/6 with positive pelvic lymph nodes). There was no detectable BrdUrd within the macroscopic tumors that expressed synaptophysin, Foxa1, Foxa2, and SV40-Tag, and these tumors had weak-to-undetectable levels of AR and did not express serotonin. In prostates without macroscopic tumors, the entire ventral prostate was paraffin-embedded and sectioned, and sections at 25-μm intervals were stained for synaptophysin and Foxa2 to identify intraglandular foci that expressed synaptophysin and/or Foxa2. The five ventral prostates harvested from intact animals that lacked macroscopic tumors contained two separate intraglandular foci that expressed synaptophysin and Foxa2 (2/5 prostates). In contrast, the three ventral prostates from castrated animals that lacked macroscopic tumors contained six independent intraglandular foci that

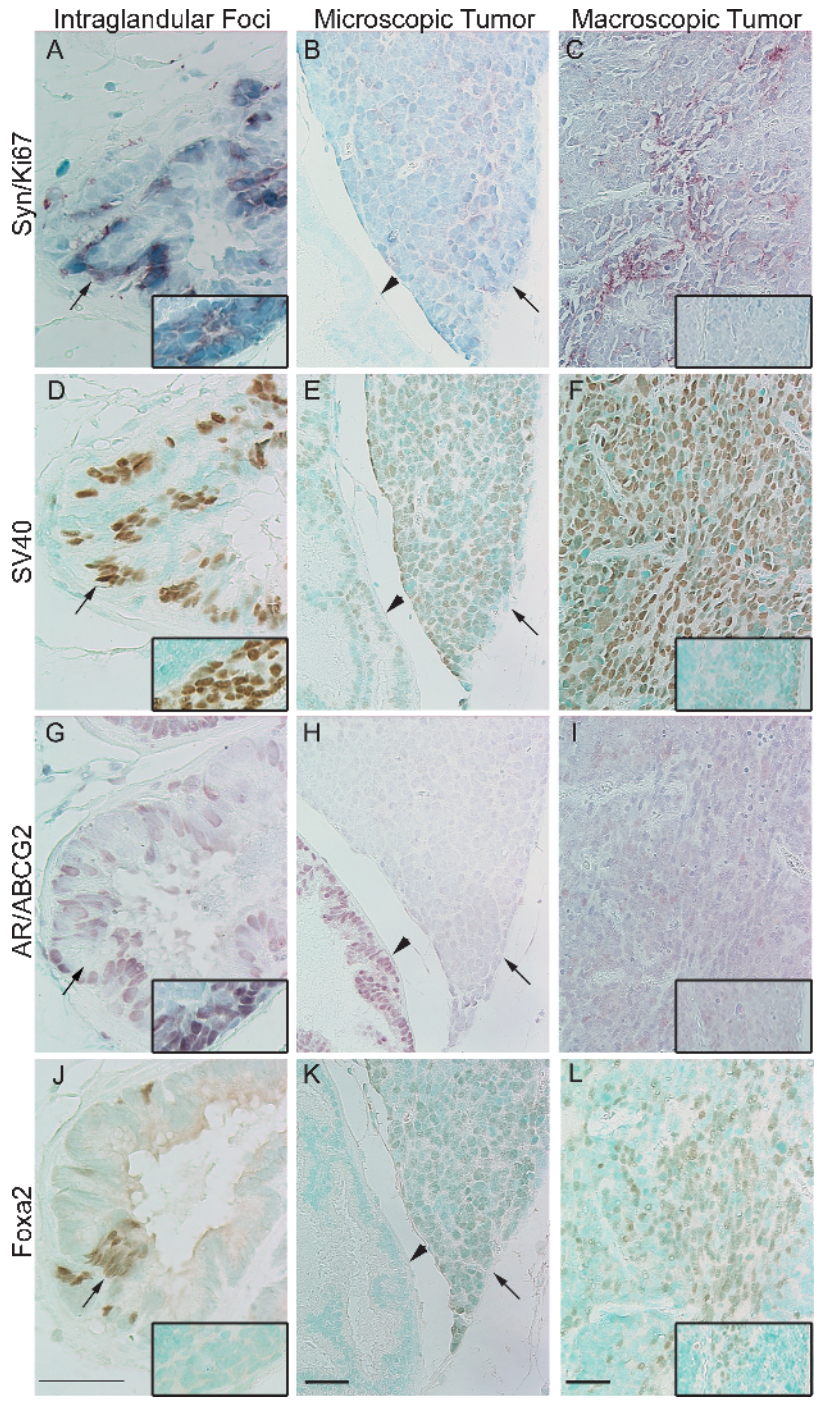

Figure 5. *Synaptophysin-expressing intraglandular foci and tumors in ventral prostate from 14- to 16-week-old intact TRAMP mice. Intraglandular synaptophysin-expressing foci (black arrow) with lymph node metastasis (inset) (A, D, G, and J); Microscopic tumor (black arrow) (B, E, H, and K); and Macroscopic tumor with lymph node metastasis (inset) (C, F, I, and L) immunostained for synaptophysin – red and Ki67 – blue (A–C); SV40-Tag – brown (D–F); AR – red and ABCG2 – blue (G–I); and Foxa2 – brown (J–L). Arrows indicate synaptophysin-, SV40-Tag–, and Foxa2-expressing intraglandular foci. Arrowheads indicate synaptophysin- and Foxa2-negative cells. Scale bar, 20 μm.*

expressed synaptophysin and Foxa2 foci (6/3 prostates). Figure 7 (*A–D*) shows serial sections of a representative intraglandular, synaptophysin- and Foxa2-expressing focus that had BrdUrd label–retaining cells located on the periphery of the foci. All synaptophysin-expressing intraglandular foci and macroscopic tumors expressed Foxa1, Foxa2, and SV40-Tag, but not AR. In cells that expressed AR, but not synaptophysin or SV40-Tag, AR was consistently nuclear in localization (Figure 7*C*). All BrdUrd-labeled cells (Figure 7*A*) represent cells that proliferated during the 14 days postcastration, but were not proliferatively active during the 14-day chase period. BrdUrd-positive cells were not detected within synaptophysin-expressing foci, but were frequently observed peripheral to the foci, suggesting that synaptophysin-expressing foci derive from postcastration label–retaining cells.

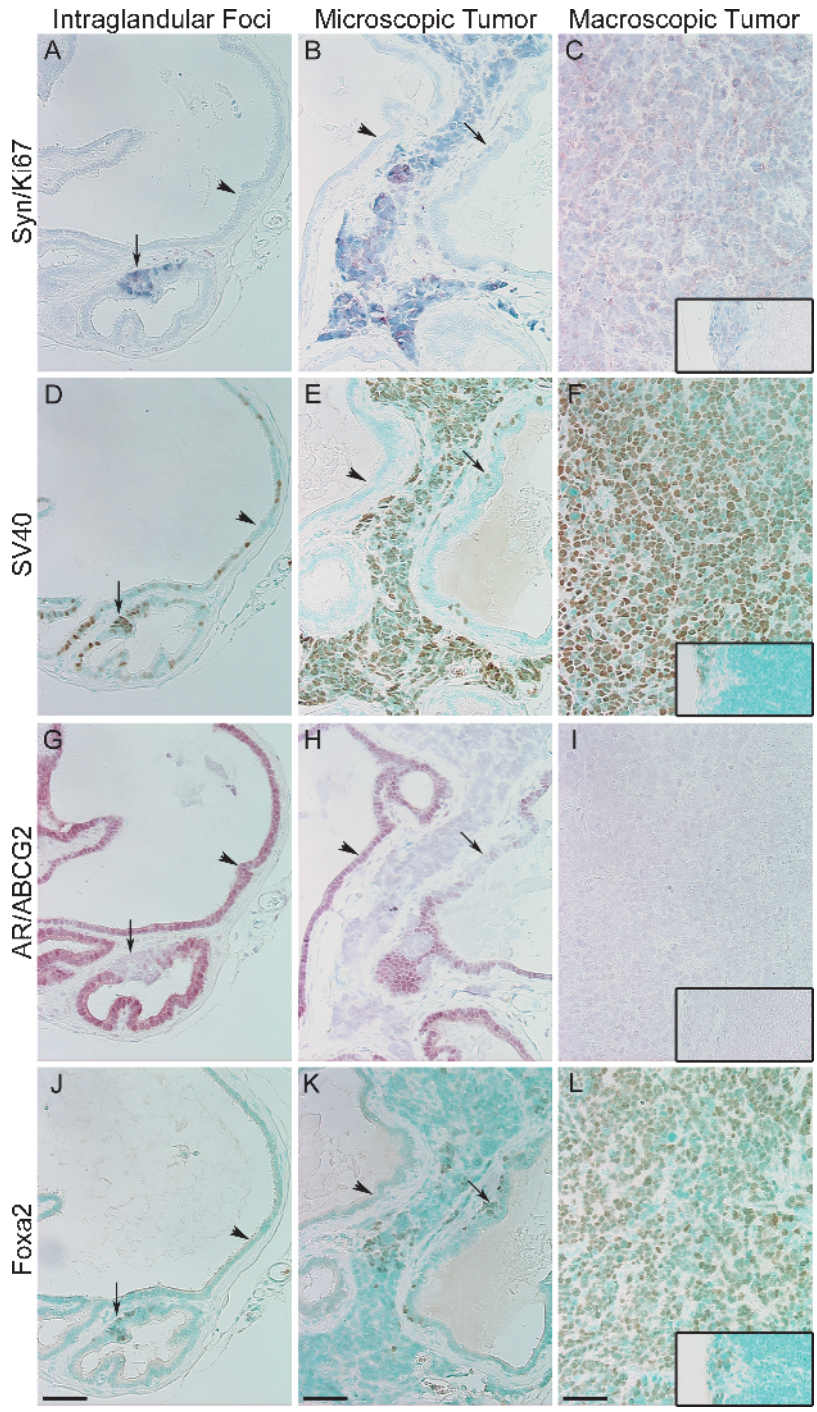

Figure 6. *Synaptophysin-expressing intraglandular foci and tumors in ventral prostate from castrated TRAMP mice. Intraglandular synaptophysin-expressing foci Day 4 postcastration (black arrow) (A, D, G, and J); Microscopic tumor Day 14 postcastration, black arrow; synaptophysin-expressing intraglandular foci (B, E, H, and K); and Macroscopic tumor Day 7 postcastration with lymph node metastasis (inset) (C, F, I, and L) immunostained for synaptophysin – red and Ki67 – blue (A–C); SV40-Tag – brown (D–F); AR – red and ABCG2 – blue (G–I); and Foxa2 – brown (J–L). Arrows indicate synaptophysin-, SV40-Tag–, and Foxa2-expressing intraglandular foci. Arrowheads indicate synaptophysin- and Foxa2-negative areas. Scale bar, 20 μm.*

Discussion

The effects of castration on multiple cellular compartments, the luminal and tumor epithelial cells and endothelial cells, of the TRAMP prostate were characterized to identify changes that occur in castrate prostates that may serve as a model of mechanisms that support the emergence of castration-recurrent prostate cancer in humans. In previous studies in the rodent prostate, the apoptotic death of secretory/luminal epithelial cells, 3 to 5 days following androgen ablation, were suggested to be a consequence of changes in the prostate stroma or in the prostate vasculature [35–37]. In TRAMP, we observed increased epithelial cell apoptosis between Days 1 and 4 postcastration; however, there was no decrease in blood vessel density or perimeter during this interval. In addition, SV40-Tag–expressing luminal epithelial cells in PIN lesions and well-differentiated adenocarcinomas in TRAMP

Table 3. Comparison of Blood Vessel Density, Proliferation, and Apoptosis between Intraglandular Synaptophysin-Expressing Foci and Microscopic or Macroscopic TRAMP Prostate Tumors.

	Intraglandular Synaptophysin$^+$ Foci		Micro- or Macroscopic Tumors	
	Intact	Cx	Intact	Cx
Blood Vessel Density	NA	NA	8.27 ± 1.05	6.133 ± 0.84
Blood Vessel Perimeter (μm/Field)	NA	NA	153.80 ± 38.9	113.42 ± 10.3
Proliferation Index (%)	50.7 ± 17.7	64.8 ± 16.6	77.6 ± 12.3	88.6 ± 8.9
Apoptosis Index (%)	0.48 ± 0.4	0.1 ± 0.05	1.3 ± 0.4	1.2 ± 0.4

lose SV40-Tag expression almost completely by Day 7 postcastration, indicating that transgene expression was regulated by androgens in both differentiated luminal cells and adenocarcinoma cells, consistent with previous reports [38]. Involution of TRAMP prostate epithelial cells occurred more rapidly than reported previously in nontransgenic rodent prostates, with the difference possibly due either to the higher number of epithelial cells in the TRAMP prostate or to the rapid loss of expression of the AR-regulated SV40-Tag protein that produces immortalization and expansion of the SV40-Tag expressing cells into adenocarcinomas.

The selective emergence of intraglandular foci of poorly differentiated cancers comprised of synaptophysin- and Foxa2-expressing cells in the castrate animals could be driven by Foxa2 transactivation of the probasin promoter of the SV40-Tag in the androgen-deprived prostates [6]. Foxa2, therefore, could substitute for the loss of AR-mediated transcription of SV40-Tag in the emerging synaptophysin-expressing foci. Foxa2 is required for the determination of endoderm cell fate and is one of the earliest differentiation markers expressed during endodermal development [39]. Furthermore, Foxa2 is expressed both in nascent prostate buds during the early stages of organogenesis [40] and in advanced stage prostate cancers, including small cell carcinoma of the prostate [6]. Therefore, Foxa2 may mediate expression of the SV40-Tag transgene in a malignantly transformed progenitor cell, or transit-amplifying cell, determining the expansion of synaptophysin-expressing foci into macroscopic tumors and metastases in the absence of androgen. Whereas SV40-Tag expression under the regulation of Foxa2 in progenitor cells may drive emergence of poorly differentiated (NE-like) cancers, SV40-Tag expression under the regulation of AR in secretory epithelial cells does not drive progression of androgen-stimulated adenocarcinomas to castration-recurrent, poorly differentiated prostate cancers, further suggesting that poorly differentiated tumors and adenocarcinomas have different origins. The emergence of these poorly differentiated foci, therefore, may provide a valuable model for the analysis of the role in recurrence of modulation of the prostate microenvironment by androgen-deprivation.

AR *versus* Foxa2 regulation of the minimal probasin promoter determines the response of the SV40-Tag expressing cell to castration. The benign luminal epithelial cells and adenocarcinoma cells depend on androgen for SV40-Tag expression, and immortalization/tumorigenicity is lost when androgen stimulation is ablated by castration. The loss of SV40-Tag expression in the AR-expressing adenocarcinoma cells in response to castration was associated with decreased proliferation and increased apoptosis. Furthermore, luminal epithelial cells that survived castration and regained AR nuclear expression by Day 14 postcastration did not regain expression of SV40-Tag. In contrast, Foxa2- and synaptophysin-expressing cells did not respond to castration; they maintained SV40-Tag expression and demonstrated no change in proliferation or apoptosis. In fact, it is possible that the AR- and SV40-Tag–expressing well-differentiated adenocarcinoma cells suppress progression of synaptophysin-expressing foci in intact TRAMP, and castration-induced regression of the androgen-stimulated adenocarcinoma cells allows the progression of the synaptophysin-expressing foci. The change in regulation of SV40-Tag expression from AR to Foxa2 may drive expansion of the NE-like, poorly differentiated cancers in the androgen-deprived environment.

BrdUrd label–retaining experiments were designed to differentiate the three possible origins for the synaptophysin-expressing foci of poorly differentiated cancers that progressed rapidly in the androgen-deprived environment of the castrate prostate. A BrdUrd pulse for 2 weeks in intact animals labeled proliferating tumor cells and facilitated testing the hypothesis that foci of poorly differentiated tumors resulted from transdifferentiation of an adenocarcinoma cell into a NE cell in response to castration, without requiring proliferative intermediates. The postmitotic NE cell would express NE markers and retain BrdUrd through the chase period following castration. Alternatively, tumor cells in foci that expressed NE markers could represent the progeny of a label-retaining cell. The slowly self-renewing cancer stem cell presumably would retain BrdUrd; however, their progeny would dilute rapidly the incorporated BrdUrd label on entering the transit-amplifying compartment which may or may not express NE markers, before initiating expression of the differentiation-associated NE markers. In TRAMP, BrdUrd label was not detected in isolated synaptophysin-expressing cells on Day 1 or 2 postcastration, therefore, it does not appear that transdifferentiation occurred immediately postcastration in the TRAMP model, as was observed in the PC-295 and PC-310 human prostate cancer xenografts [26,27,41]. Furthermore, the highly proliferative intraglandular synaptophysin-expressing foci were detected at a similar frequency in sham-castrated mice and in castrated mice, suggesting that the foci were present before castration. Our studies support the hypothesis that transactivation of SV40-Tag by Foxa2 in a tumor progenitor cell drives expansion of the poorly differentiated foci in the absence of androgen and suggest that changes in the environment of these cells determine the probability and kinetics of their progression to macroscopic tumors.

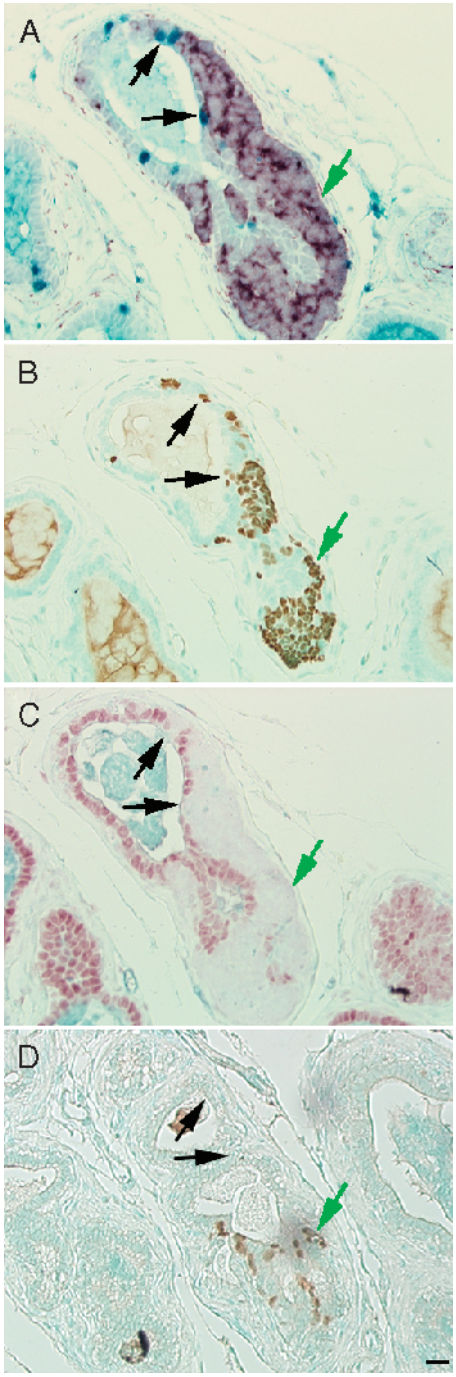

Figure 7. *BrdUrd label–retaining cells following castration. BrdUrd implanted at the time of castration at 14 weeks of age and BrdUrd was removed at 16 weeks of age, serial prostate sections were immunostained following 5 weeks of castration and 3 weeks of BrdUrd removal for BrdUrd – blue and synaptophysin – red (A); SV40-Tag – brown (B); AR – red and ABCG2 – blue (C); or Foxa2 – brown (D). Black arrows indicate BrdUrd label–retaining cells. Green arrows indicate synaptophysin-expressing cells postcastration. Scale bar, 20 μm.*

A tumor stem cell model for the etiology and progression of prostate cancer is consistent with the predictable emergence of these foci of poorly differentiated cancer in TRAMP and castration-recurrent prostate cancer in humans. In a tumor stem cell–driven model of cancer, a small population of tumor stem cells escapes tissue microenvironmental constraints on self-renewal, as well as therapeutic regimens including androgen-deprivation therapy, and gives rise to progeny that abnormally/incompletely/aberrantly differentiate (express synaptophysin) in response to the presence/absence of microenvironmental signals. The tendency of prostate cells to acquire NE characteristics on androgen-deprivation may indicate that differentiation toward a NE lineage represents a default survival mechanism of prostate stem cell progeny. Potential markers for prostate stem cells and/or prostate tumor stem cells are currently being investigated by several groups. Xin et al. [42] have proposed that Sca-1 expression marks the prostate-regenerating cell in the mouse. Sca-1–expressing prostate-regenerating cells represented approximately 30% of cells in proximal regions of prostate tubules and 10% of cells in the distal tips, and the relative percent of Sca-1$^+$ cells increased to 70% after castration [42]. Furthermore, Sca-1–expressing cells regenerated whole tubular structures in tissue recombination studies with rat urogenital mesenchyme [42]. Schalken and van Leenders [43] have proposed that prostate stem cells can be identified by expression of intermediate patterns of cytokeratins that reflect all of the potential differentiated progeny of the stem cell. The least differentiated stem cells are proposed to express cytokeratin 5 and cytokeratin 14, with weak expression of cytokeratin 18 [43]. Intermediate stages of differentiation by the progeny of the stem cells that have exited the stem cell compartment are indicated by expression of cytokeratin 5, cytokeratin 18, c-met, α_2-integrin, and inducible laminin-γ_2 [43]. Malignant transformation of an intermediate cell would explain how prostate cancer cells express markers of both secretory (cytokeratin) and neuroendocrine (chromogranin A) differentiation. Finally, several groups of investigators have proposed that the prostate stem cell is typified by coexpression of a group of markers, CD44$^+$/$\alpha_2\beta_1^{hi}$/CD133$^+$ [44,45]. These markers identify approximately 0.1% of epithelial cells in benign prostate and prostate cancer, and only CD133$^+$ cells isolated from tumors were capable of self-renewal and extensive proliferation [45]. The CD44$^+$/$\alpha_2\beta_1^{hi}$/CD133$^+$ cell population, when engrafted with human prostate stromal cells, gave rise to cytokeratin 8/prostatic acid phosphatase/AR-expressing xenografts; loss of CD133 may indicate relocation to the transit-amplifying compartment and loss of the stem cell phenotype [44]. We reported recently that the prostate stem cell and prostate tumor stem cell in mouse, rat, and humans was characterized by expression of the ATP-binding cassette transporter family membrane efflux pump ABCG2 (BCRP) and by lack of AR protein [32]. Cells that coexpressed ABCG2 and the SV40-Tag transgene were not observed in prostates from TRAMP mice. The lack of expression of SV40-Tag in the putative stem cell could be due to the lack of expression of AR or Foxa2 in the ABCG2-expressing cells. Expression of AR in stem cell progeny could be correlated with commitment to differentiation along a luminal epithelial lineage, whereas expression of Foxa2 in stem cell progeny could be correlated with commitment to NE differentiation.

This study suggests that the majority of the macroscopic, poorly differentiated tumors that represent the lethal phenotype in TRAMP are independent of, and not a progression

from, the PIN and well-differentiated adenocarcinomas that are a result of AR-mediated, SV40-Tag transgene expression in secretory epithelial cells. The rare, poorly differentiated, primary and metastatic tumors that express synaptophysin support an origin from a transformed transit-amplifying cell committed to a NE lineage, with SV40-Tag driving the tumorigenic phenotype under the regulation of Foxa2 upregulated in the absence of AR [4]. The potential of TRAMP to model a transformed transit-amplifying and or intermediate cell resulting in androgen-insensitive prostate cancer would provide a valuable tool for the identification and characterization of the prostate cancer stem cell and lead to a preclinical tool for testing therapies designed to target the prostate cancer stem cell.

Acknowledgements

We thank Courtney Abshier, Brian Buckley, Deirdre Buckley, Manish Dayal, and Sinisa Haberle for technical assistance and Caroline Castile for animal assistance.

References

[1] Ahlgren G, Pedersen K, Lundberg S, Aus G, Hugosson J, and Abrahamsson PA (2000). Regressive changes and neuroendocrine differentiation in prostate cancer after neoadjuvant hormonal treatment. *Prostate* **42**, 274–279.

[2] Aprikian AG, Cordon-Cardo C, Fair WR, Zhang ZF, Bazinet M, Hamdy SM, and Reuter VE (1994). Neuroendocrine differentiation in metastatic prostatic adenocarcinoma. *J Urol* **151**, 914–919.

[3] Segawa N, Mori I, Utsunomiya H, Nakamura M, Nakamura Y, Shan L, Kakudo K, and Katsuoka Y (2001). Prognostic significance of neuroendocrine differentiation, proliferation activity and androgen receptor expression in prostate cancer. *Pathol Int* **51**, 452–459.

[4] Evangelou AI, Winter SF, Huss WJ, Bok RA, and Greenberg NM (2004). Steroid hormones, polypeptide growth factors, hormone refractory prostate cancer, and the neuroendocrine phenotype. *J Cell Biochem* **91**, 671–683.

[5] Kaplan-Lefko PJ, Chen TM, Ittmann MM, Barrios RJ, Ayala GE, Huss WJ, Maddison LA, Foster BA, and Greenberg NM (2003). Pathobiology of autochthonous prostate cancer in a pre-clinical transgenic mouse model. *Prostate* **55**, 219–237.

[6] Mirosevich J, Gao N, Gupta A, Shappell SB, Jove R, and Matusik RJ (2006). Expression and role of Foxa proteins in prostate cancer. *Prostate* **66**, 1013–1028.

[7] Wiedenmann B (1991). Synaptophysin. A widespread constituent of small neuroendocrine vesicles and a new tool in tumor diagnosis. *Acta Oncol* **30**, 435–440.

[8] Shappell SB, Thomas GV, Roberts RL, Herbert R, Ittmann MM, Rubin MA, Humphrey PA, Sundberg JP, Rozengurt N, Barrios R, et al. (2004). Prostate pathology of genetically engineered mice: definitions and classification. The consensus report from the Bar Harbor meeting of the Mouse Models of Human Cancer Consortium Prostate Pathology Committee. *Cancer Res* **64**, 2270–2305.

[9] Johnson MA, Iversen P, Schwier P, Corn AL, Sandusky G, Graff J, and Neubauer BL (2005). Castration triggers growth of previously static androgen-independent lesions in the transgenic adenocarcinoma of the mouse prostate (TRAMP) model. *Prostate* **62**, 322–338.

[10] Gingrich JR, Barrios RJ, Kattan MW, Nahm HS, Finegold MJ, and Greenberg NM (1997). Androgen-independent prostate cancer progression in the TRAMP model. *Cancer Res* **57**, 4687–4691.

[11] Eng MH, Charles LG, Ross BD, Chrisp CE, Pienta KJ, Greenberg NM, Hsu CX, and Sanda MG (1999). Early castration reduces prostatic carcinogenesis in transgenic mice. *Urology* **54**, 1112–1119.

[12] Wikstrom P, Lindahl C, and Bergh A (2005). Characterization of the autochthonous transgenic adenocarcinoma of the mouse prostate (TRAMP) as a model to study effects of castration therapy. *Prostate* **62**, 148–164.

[13] Kaplan PJ, Mohan S, Cohen P, Foster BA, and Greenberg NM (1999). The insulin-like growth factor axis and prostate cancer: lessons from the transgenic adenocarcinoma of mouse prostate (TRAMP) model. *Cancer Res* **59**, 2203–2209.

[14] Huss WJ, Hanrahan CF, Barrios RJ, Simons JW, and Greenberg NM (2001). Angiogenesis and prostate cancer: identification of a molecular progression switch. *Cancer Res* **61**, 2736–2743.

[15] Huss WJ, Barrios RJ, Foster BA, and Greenberg NM (2003). Differential expression of specific FGF ligand and receptor isoforms during angiogenesis associated with prostate cancer progression. *Prostate* **54**, 8–16.

[16] Uzgare AR, Kaplan PJ, and Greenberg NM (2003). Differential expression and/or activation of P38MAPK, erk1/2, and jnk during the initiation and progression of prostate cancer. *Prostate* **55**, 128–139.

[17] Maddison LA, Huss WJ, Barrios RM, and Greenberg NM (2004). Differential expression of cell cycle regulatory molecules and evidence for a "cyclin switch" during progression of prostate cancer. *Prostate* **58**, 335–344.

[18] di Sant'Agnese PA (2001). Neuroendocrine differentiation in prostatic carcinoma: an update on recent developments. *Ann Oncol* **12** (Suppl 2), S135–S140.

[19] Casella R, Bubendorf L, Sauter G, Moch H, Mihatsch MJ, and Gasser TC (1998). Focal neuroendocrine differentiation lacks prognostic significance in prostate core needle biopsies. *J Urol* **160**, 406–410.

[20] Bonkhoff H (1998). Neuroendocrine cells in benign and malignant prostate tissue: morphogenesis, proliferation, and androgen receptor status. *Prostate Suppl* **8**, 18–22.

[21] Burchardt T, Burchardt M, Chen MW, Cao Y, de la Taille A, Shabsigh A, Hayek O, Dorai T, and Buttyan R (1999). Transdifferentiation of prostate cancer cells to a neuroendocrine cell phenotype *in vitro* and *in vivo*. *J Urol* **162**, 1800–1805.

[22] Bang YJ, Pirnia F, Fang WG, Kang WK, Sartor O, Whitesell L, Ha MJ, Tsokos M, Sheahan MD, Nguyen P, et al. (1994). Terminal neuroendocrine differentiation of human prostate carcinoma cells in response to increased intracellular cyclic AMP. *Proc Natl Acad Sci USA* **91**, 5330–5334.

[23] Shen R, Dorai T, Szaboles M, Katz AE, Olsson CA, and Buttyan R (1997). Transdifferentiation of cultured human prostate cancer cells to a neuroendocrine cell phenotype in a hormone-depleted medium. *Urol Oncol* **3**, 67–75.

[24] Cox ME, Deeble PD, Lakhani S, and Parsons SJ (1999). Acquisition of neuroendocrine characteristics by prostate tumor cells is reversible: implications for prostate cancer progression. *Cancer Res* **59**, 3821–3830.

[25] Noordzij MA, van Weerden WM, de Ridder CM, van der Kwast TH, Schroder FH, and van Steenbrugge GJ (1996). Neuroendocrine differentiation in human prostatic tumor models. *Am J Pathol* **149**, 859–871.

[26] Jongsma J, Oomen MH, Noordzij MA, Van Weerden WM, Martens GJ, van der Kwast TH, Schroder FH, and van Steenbrugge GJ (1999). Kinetics of neuroendocrine differentiation in an androgen-dependent human prostate xenograft model. *Am J Pathol* **154**, 543–551.

[27] Jongsma J, Oomen MH, Noordzij MA, Van Weerden WM, Martens GJ, van der Kwast TH, Schroder FH, and van Steenbrugge GJ (2002). Different profiles of neuroendocrine cell differentiation evolve in the PC-310 human prostate cancer model during long-term androgen deprivation. *Prostate* **50**, 203–215.

[28] Tsujimura A, Koikawa Y, Salm S, Takao T, Coetzee S, Moscatelli D, Shapiro E, Lepor H, Sun TT, and Wilson EL (2002). Proximal location of mouse prostate epithelial stem cells: a model of prostatic homeostasis. *J Cell Biol* **157**, 1257–1265.

[29] Bonkhoff H (2001). Neuroendocrine differentiation in human prostate cancer. Morphogenesis, proliferation and androgen receptor status. *Ann Oncol* **12** (Suppl 2), S141–S144.

[30] Rumpold H, Heinrich E, Untergasser G, Hermann M, Pfister G, Plas E, and Berger P (2002). Neuroendocrine differentiation of human prostatic primary epithelial cells *in vitro*. *Prostate* **53**, 101–108.

[31] Huang J, Yao JL, di Sant'Agnese PA, Yang Q, Bourne PA, and Na Y (2006). Immunohistochemical characterization of neuroendocrine cells in prostate cancer. *Prostate* **66**, 1399–1406.

[32] Huss WJ, Gray DR, Greenberg NM, Mohler JL, and Smith GJ (2005). Breast cancer resistance protein-mediated efflux of androgen in putative benign and malignant prostate stem cells. *Cancer Res* **65**, 6640–6650.

[33] Jonker JW, Buitelaar M, Wagenaar E, Van Der Valk MA, Scheffer GL, Scheper RJ, Plosch T, Kuipers F, Elferink RP, Rosing H, et al. (2002). The breast cancer resistance protein protects against a major chlorophyll-derived dietary phototoxin and protoporphyria. *Proc Natl Acad Sci USA* **99**, 15649–15654.

[34] O'Neill RR, Mitchell LG, Merril CR, and Rasband WS (1989). Use of image analysis to quantitate changes in form of mitochondrial DNA after X-irradiation. *Appl Theor Electrophor* **1**, 163–167.

[35] Kurita T, Wang YZ, Donjacour AA, Zhao C, Lydon JP, O'Malley BW, Isaacs JT, Dahiya R, and Cunha GR (2001). Paracrine regulation of apoptosis by steroid hormones in the male and female reproductive system. *Cell Death Differ* **8**, 192–200.

[36] Lekas E, Johansson M, Widmark A, Bergh A, and Damber JE (1997). Decrement of blood flow precedes the involution of the ventral prostate in the rat after castration. *Urol Res* **25**, 309–314.

[37] Buttyan R, Shabsigh A, Perlman H, and Colombel M (1999). Regulation of apoptosis in the prostate gland by androgenic steroids. *Trends Endocrinol Metab* **10**, 47–54.

[38] Greenberg NM, DeMayo FJ, Sheppard PC, Barrios R, Lebovitz R, Finegold M, Angelopoulou R, Dodd JG, Duckworth ML, Rosen JM, et al. (1994). The rat probasin gene promoter directs hormonally and developmentally regulated expression of a heterologous gene specifically to the prostate in transgenic mice. *Mol Endocrinol* **8**, 230–239.

[39] Monaghan AP, Kaestner KH, Grau E, and Schutz G (1993). Postimplantation expression patterns indicate a role for the mouse forkhead/HNF-3 alpha, beta and gamma genes in determination of the definitive endoderm, chordamesoderm and neuroectoderm. *Development* **119**, 567–578.

[40] Mirosevich J, Gao N, and Matusik RJ (2005). Expression of Foxa transcription factors in the developing and adult murine prostate. *Prostate* **62**, 339–352.

[41] Jongsma J, Oomen MH, Noordzij MA, Van Weerden WM, Martens GJ, van der Kwast TH, Schroder FH, and van Steenbrugge GJ (2000). Androgen deprivation of the PC-310 [correction of prohormone convertase-310] human prostate cancer model system induces neuroendocrine differentiation. *Cancer Res* **60**, 741–748.

[42] Xin L, Lawson DA, and Witte ON (2005). The Sca-1 cell surface marker enriches for a prostate-regenerating cell subpopulation that can initiate prostate tumorigenesis. *Proc Natl Acad Sci USA* **102**, 6942–6947.

[43] Schalken JA and van Leenders G (2003). Cellular and molecular biology of the prostate: stem cell biology. *Urology* **62**, 11–20.

[44] Rizzo S, Attard G, and Hudson DL (2005). Prostate epithelial stem cells. *Cell Prolif* **38**, 363–374.

[45] Collins AT, Berry PA, Hyde C, Stower MJ, and Maitland NJ (2005). Prospective identification of tumorigenic prostate cancer stem cells. *Cancer Res* **65**, 10946–10951.

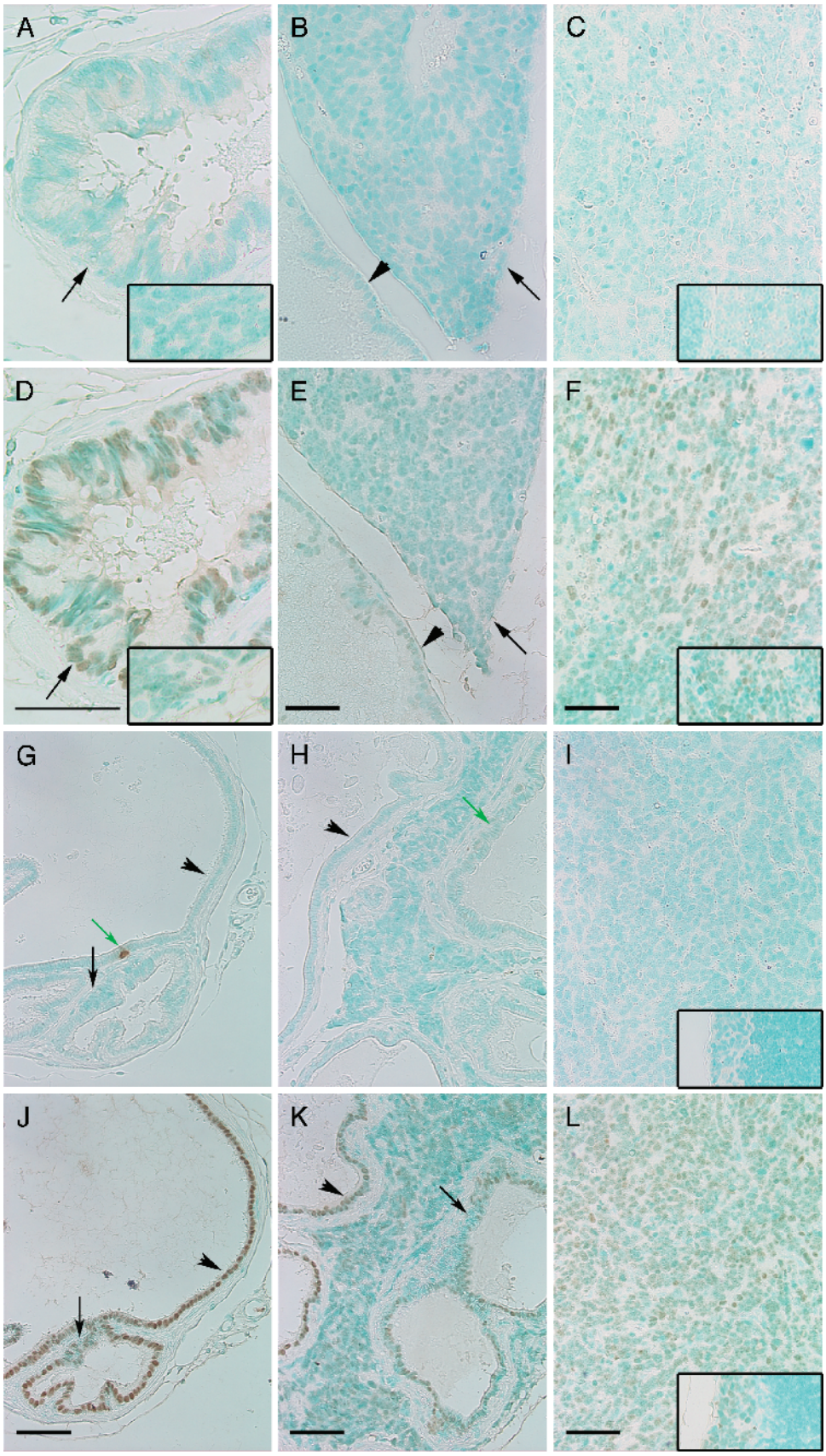

Figure W1. *Serial sections from Figures 5 and 6 of intraglandular foci, microscopic, and macroscopic tumors from intact TRAMP mice (A–F) and castrated TRAMP mice (G–L). Serial sections were immunostained for serotonin (A–C; G–I) or Foxa1 (D–F; J–L). Arrows indicate synaptophysin-, SV40-Tag–, and Foxa2-expressing intraglandular foci. Arrowheads indicate synaptophysin- and Foxa2-negative areas. Green arrow indicates serotonin-expressing cell. Scale bar, 20 μm.*